Vertical Grids and Upper Boundary Conditions

Learning Outcomes

Following this lecture, students will be able to:

- Understand the key physical considerations for choosing a model vertical coordinate.
- Describe strengths and weaknesses of constant height, constant pressure, constant potential temperature, and terrain-following vertical coordinates.
- Describe the importance of maintaining consistency between horizontal and vertical grid spacing (or resolution) in numerical simulations.
- Describe special considerations associated with how the model's upper boundary is represented.

Introduction to Vertical Coordinate Systems

Numerical models can be formulated with one of many vertical coordinates, with the primitive equations' partial derivatives in the vertical direction transformed to this vertical coordinate. However, a given model is typically based on a single vertical coordinate. This, a model user does not have the ability to choose the vertical coordinate apart from choosing the model.

There are three primary considerations to vertical coordinates:

- **Does the chosen vertical coordinate system permit unevenly distributed vertical levels?** Nearly all numerical models used for real-data simulations allow for unevenly distributed vertical levels, and strictly speaking this consideration lies with the model itself and not with the choice of vertical coordinate. By contrast, some models used for idealized simulations only permit a fixed distribution – with constant spacing – between vertical levels.

  Variable vertical resolution allows for more levels to be placed at altitudes where sharp vertical gradients in meteorological quantities exist, such as the boundary layer, without having to add more vertical levels throughout the atmosphere.

- **What is the relationship between the chosen vertical coordinate system and terrain?** In models with sloping terrain, it is possible for the vertical surfaces of selected vertical coordinate systems to intersect the terrain. This poses a computational challenge that must be addressed in some fashion to ensure robust results. We prefer that vertical coordinate surfaces not intersect the ground; i.e., that they follow the terrain.

- **In transforming the horizontal pressure gradient terms in the momentum equations to the chosen vertical coordinate system, do one or two terms result?** While it is fairly straightforward to transform the terms in the primitive equations between chosen vertical coordinate systems, the transformation itself can result in an added term.

  For example, when we introduced the WRF-ARW model equations, we transformed the horizontal pressure gradient term in the *u*-momentum equation from constant height surfaces to the terrain-following η vertical coordinate used by the WRF-ARW model:

  $$-\frac{1}{\rho}\frac{\partial p}{\partial x}_z \qquad\qquad -\alpha\mu_d \frac{\partial p}{\partial x}_\eta \; -\frac{\alpha}{\alpha_d}\frac{\partial p}{\partial \eta}\frac{\partial \Phi}{\partial x}_\eta$$

  (constant height) (terrain-following, coupled to the dry air mass)

  Adding an extra partial derivative to be approximated using finite differences adds another source of truncation error to the model. This is particularly troublesome for horizontal pressure gradient terms since truncation errors in computing the horizontal pressure gradient can be of similar magnitude to horizontal variability in the horizontal pressure gradient itself. Modern models such as WRF-ARW typically address this by recasting pressure, geopotential height, and dry-air mass into their perturbation forms, so that the terms themselves and the associated truncation errors are smaller. However, generally speaking, we prefer to not add partial derivative terms.

We now wish to consider the strengths and weaknesses of several vertical coordinate systems in light of the aforementioned considerations.

Height Above Sea Level – Constant Height (z) Coordinate

This coordinate is perhaps the most intuitive: sea level is at a height $z = 0$, and the height z increases with increasing distance above sea level. It is the vertical coordinate that we are first introduced to when considering the primitive equations as undergraduate students.

The horizontal pressure gradient term in this vertical coordinate is of the form:

$$-\frac{1}{\rho}\nabla_z p$$

where the subscript of z on the gradient operator indicates that it is applied on a constant height surface. There is only one horizontal pressure gradient term in the *u*- and *v*-momentum equations when formulated on constant height surfaces. Thus, our third criterion above is met.

This vertical coordinate system poses no intrinsic inhibition against having unevenly distributed vertical levels, such that it meets our first criterion above so long as the model permits unevenly distributed vertical levels.

This leaves our second criterion. An example of unevenly distributed height surfaces relative to a hypothetical sloping terrain is given in Fig. 1. This figure illustrates the primary shortcoming of the constant height vertical coordinate: except for flat terrain at sea level, it is a terrain-intersecting vertical coordinate.

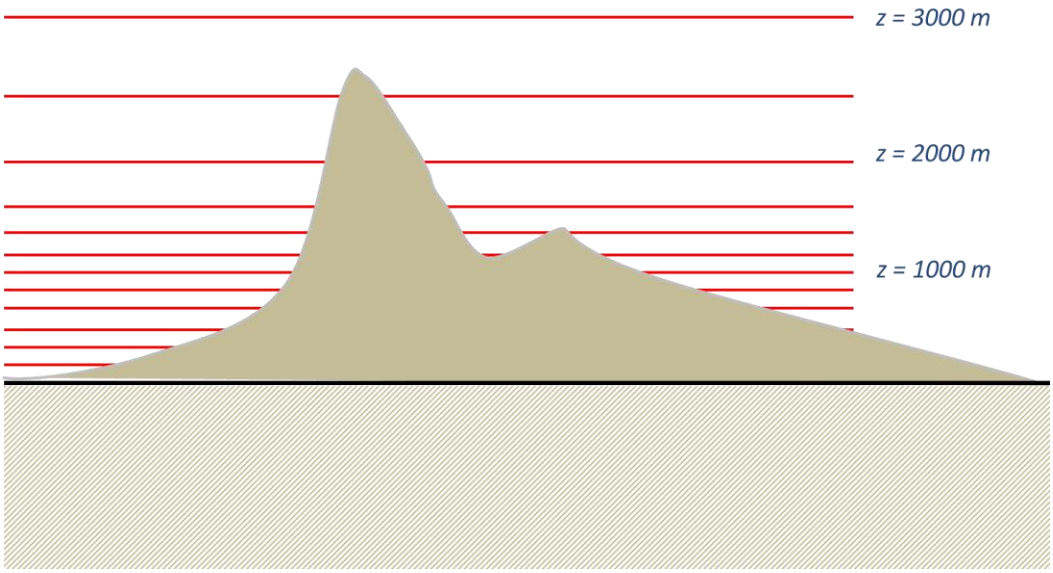

Figure 1. Hypothetical depiction of unevenly distributed constant height (z) surfaces relative to an idealized sloping terrain profile.

Consider partial derivatives in both the horizontal and vertical directions evaluated adjacent to the terrain along a constant height surface such as the z = 2000 m surface in Fig. 1. Evaluating these partial derivatives involves one or more points where atmospheric quantities are undefined due to being below ground. Furthermore, the discontinuous nature of atmospheric fields adjacent to the terrain along constant height surfaces make it impossible to evaluate horizontal partial derivatives using spectral methods with this vertical coordinate.

While there are methods to address computing partial derivatives along constant height surfaces near sloping terrain, these can be computationally expensive. Alternatively, one can use forward or backward finite differences to compute partial derivatives adjacent to sloping terrain, but these are associated with an unacceptably high amount of truncation error. Furthermore, each of these alternatives require different methods to compute the partial derivatives adjacent to terrain from those in the free atmosphere. Consequently, they pose a technical challenge to implement in a numerical model.

As a result of this shortcoming, the constant height vertical coordinate is typically not used within modern models. The primary exception to this lies with models used exclusively for idealized simulations that do not incorporate terrain information.

Pressure – Isobaric (p) Surfaces

We are also likely quite familiar with the primitive equations cast into the isobaric, or constant pressure, vertical coordinate. Pressure, a function of the mass of the air above you, is highest at the surface and decreases log-linearly with increasing distance upward from the surface.

Transforming the primitive equations to the isobaric coordinate results in only one term for the horizontal pressure gradient in each of the horizontal momentum equations. This term takes the form $\nabla_p \Phi$, where the geopotential $\Phi = gz$ and the gradient operator's subscript of p indicates that it is applied on an isobaric surface. As a result, our third criterion is met, just as it was with the z vertical coordinate.

As did the constant height vertical coordinate, the isobaric coordinate system poses no inhibition against having unevenly distributed vertical levels, such that it meets our first criterion above so long as the model itself permits such a distribution of vertical levels. An example of unevenly distributed isobaric surfaces relative to a hypothetical sloping terrain surface is given in Fig. 2.

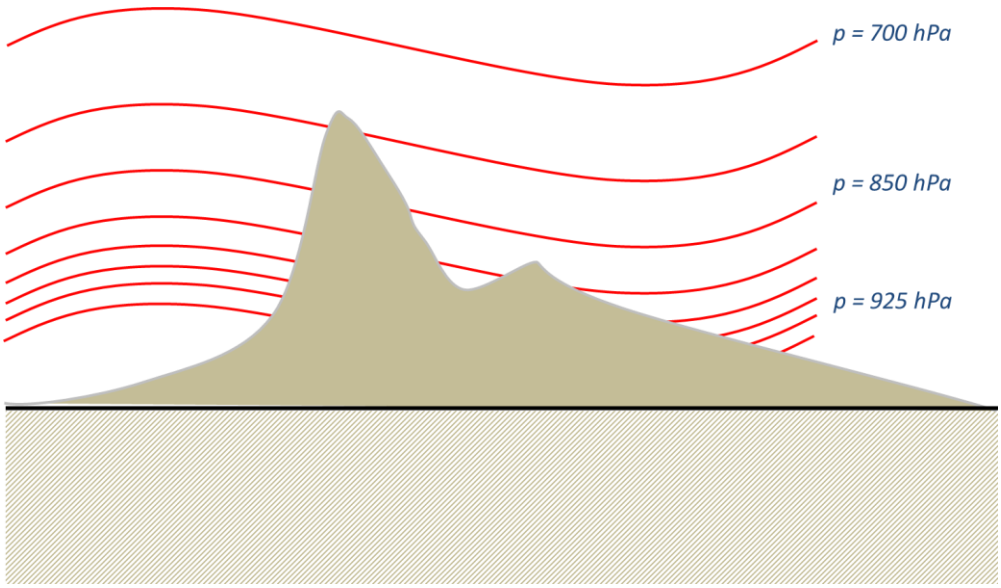

Figure 2. Hypothetical depiction of unevenly distributed isobaric surfaces relative to an idealized sloping terrain profile. The slope of the isobaric surfaces depicted here is a function of the prevailing meteorology, indicating relatively high (low) pressure to the left/west (right/east).

This figure, however, also highlights the primary shortcoming of the isobaric vertical coordinate: it is also a terrain-intersecting vertical coordinate. The same challenges with computing partial derivatives adjacent to sloping terrain noted for the height coordinate hold for the isobaric vertical coordinate for both grid-based and spectral models. The isobaric vertical coordinate poses an additional challenge, however, in that the isobaric surfaces themselves change altitude with time as a function of the prevailing meteorology. In other words, at a given horizontal grid point, a given isobaric surface may be above ground at one time but below ground at another time. As a result, the isobaric vertical coordinate is typically not used within numerical models.

Potential Temperature – Isentropic (θ) Surfaces

As an undergraduate student, you were introduced to potential temperature, which is a function of temperature *T* and pressure *p* as expressed by Poisson's equation:

$$\theta = T\left(\frac{p_0}{p}\right)^{R_d/c_p}$$

where p_0 is a reference-state pressure and is typically equal to 1000 hPa. Potential temperature typically (but not always) increases with increasing height.

Under dry-adiabatic conditions, potential temperature is conserved following the motion. This makes potential temperature an appealing vertical coordinate: flow across isentropes, which constitutes vertical motion in the isentropic vertical coordinate system, is small and only occurs when diabatic heating is occurring. If vertical motion is small, vertical advection is also small, which is also appealing since it means that truncation errors from computing vertical advection will be small.

Another benefit of the isentropic vertical coordinate is that vertical levels – i.e., isentropic surfaces – are naturally packed where vertical temperature gradients are large, such as with fronts. A representative example is given in Fig. 3. At left, a vertical cross-section from San Diego, CA to Medford, OR in isobaric coordinates is depicted. The cold front is located between 700-600 hPa near San Diego and slopes upward to the north, intersecting the tropopause between 400-300 hPa near Oakland, CA. The isentropes are tightly packed through the frontal zone. From thermal wind balance, there is also strong vertical wind shear with the front, particularly between Point Arguello, CA and Oakland, CA. Thus, there exist sharp horizontal and vertical gradients in both potential temperature and wind across the front.

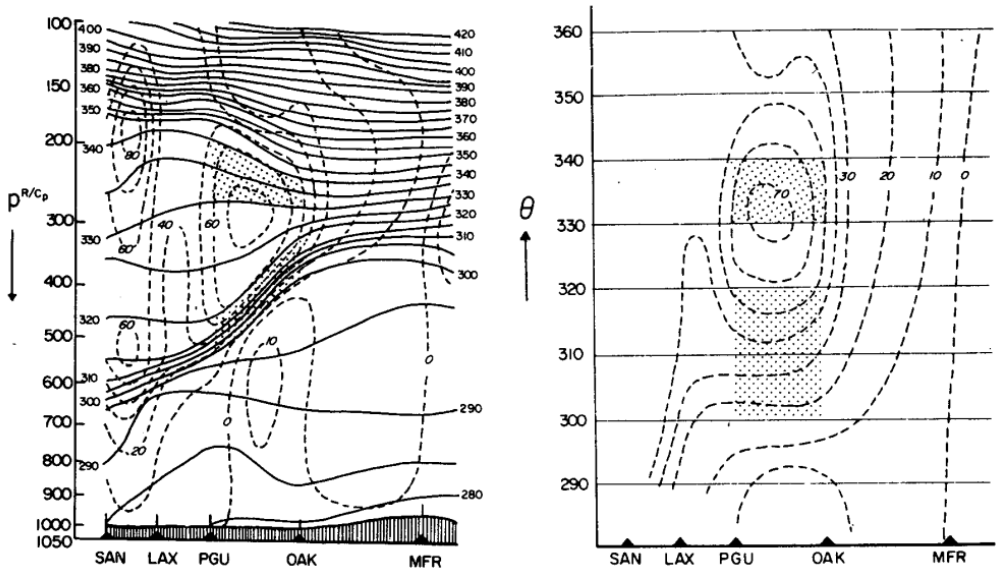

Figure 3. Vertical cross-sections (south-north) of a cold front in (left) isobaric and (right) isentropic coordinates. In both panels, isentropes (every 5 K at left, every 10 K at right) are given by the solid lines and isotachs (every 10 m s^{-1}) are given by the dashed lines. The shaded grey area in the center of each panel spans the same physical volume of atmosphere encompassed by the cold front between Point Arguello, CA and Oakland, CA. Figure reproduced from Benjamin (1989, *Mon. Wea. Rev.*), their Fig. 1.

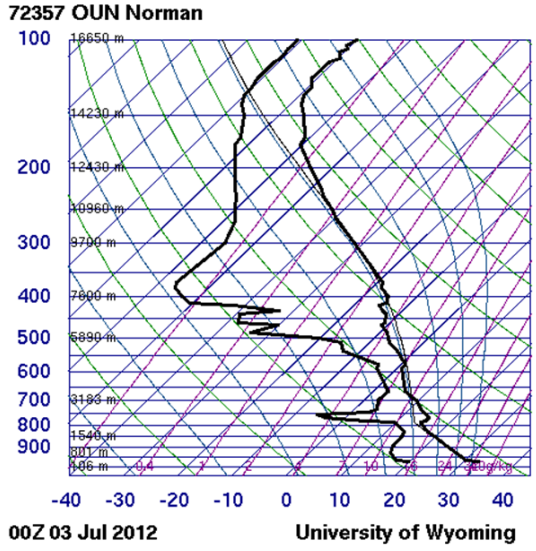

72357 OUN Norman Observations at 00Z 03 Jul 2012

PRES hPa	HGHT m	TEMP C	DWPT C	RELH %	MIXR g/kg	DRCT deg	SKNT knot	THTA K	THTE K	THTV K
1000.0	106									
973.0	345	32.8	19.8	46	15.18	170	10	308.4	354.6	311.1
964.0	430	30.2	17.2	46	12.97	170	14	306.5	345.9	308.9
944.9	610	28.6	16.0	47	12.27	170	23	306.6	343.9	308.9
925.0	801	26.8	14.8	48	11.57	175	22	306.7	341.9	308.8
913.2	914	25.8	14.5	50	11.49	175	21	306.8	341.7	308.9

Figure 4. (left) 0000 UTC 3 July 2012 skew *T*-ln *p* diagram for Norman, OK. The temperature (dewpoint temperature) trace is given by the rightmost (leftmost) thick black line. (right) Tabular display of data from below 913.2 hPa from the 0000 UTC 3 July 2012 Norman, OK skew *T*-ln *p* diagram. Note the superadiabatic lapse rate at the surface at left and the corresponding decrease in potential temperature (THTA) between 973 hPa and 964 hPa at right. Figure and data obtained from the University of Wyoming.

At right, the same data are plotted, except using an isentropic vertical coordinate system. The cold front is found between the 300-320 K isentropic surfaces, as expected from the left panel. For a chosen vertical-level distribution, this inherently allows higher vertical resolution where the sharpest gradients exist. The same is true across any temperature inversion, and thus our third criterion is met without the need to explicitly specify unevenly distributed vertical levels. This reduces the magnitudes of both horizontal and vertical wind gradients are reduced, though the coordinate transformation introduces relatively sharp horizontal gradients in height, pressure, and temperature (not shown).

There are three primary shortcomings of the isentropic vertical coordinate, however, that limit its use for numerical weather prediction:

- Where the lapse rate is greater than dry adiabatic, such as in Fig. 4, an isentropic surface is not uniquely identified with a given altitude and thus meteorological conditions. This frequently occurs with strong surface sensible heating during the local daytime hours in the warm season. While a correction term can be added to prevent the lapse rate from becoming superadiabatic, such a term is non-physical and may result in inaccurate model results near the surface.

- As with isobaric surfaces, isentropic surfaces can intersect the ground, and whether a given grid point is above or below ground can change as a function of the meteorology. This issue is arguably more common with isentropic surfaces than with isobaric surfaces given the isentropic coordinate's direct link to temperature.

- Transforming the horizontal pressure gradient term into isentropic coordinates results in the addition of a second term. Specifically, the horizontal pressure gradient term applicable on isentropic surfaces takes the form:

$$-\nabla_\theta \left(gz + c_p T \right)$$

  The subscript of θ on the gradient operator indicates that it is applied on isentropic surfaces. As sharp horizontal gradients in both z and T on an isentropic surface (such as with fronts) may exist, large truncation errors may result when finite-difference methods are used. Since these errors may not cancel, this results in a potentially large error source.

As a result of these shortcomings, isentropic vertical coordinates are rare in modern NWP.

Terrain-Following Vertical Coordinates

As we discovered with the WRF-ARW model in an earlier lecture, it is possible to utilize a terrain-following vertical coordinate. The primary advantage of doing so is to eliminate the

possibility for vertical coordinate surfaces to intersect terrain, which was a major shortcoming with the constant height, isobaric, and isentropic vertical coordinates noted above.

A generalized terrain-following vertical coordinate σ may be formulated with respect to either pressure p (left) or height z (right):

$$\sigma = \frac{p - p_t}{p_s - p_t} \qquad\qquad \sigma = \frac{z_t - z}{z_t - z_s}$$

Note that p need not be the full pressure but can be some derivative thereof, such as dry hydrostatic pressure as in the WRF-ARW model. The pressure p_t or height z_t at the top of the model is specified by the user. The surface height z_s is fixed to the terrain, whereas the surface pressure p_s can change by a small amount through the simulation as a function of the prevailing meteorology.

For both pressure- and height-based formulations, $\sigma = 0$ at the top of the model and $\sigma = 1$ at the terrain surface. The terrain influence on the coordinate surfaces' slope decreases linearly with increasing altitude.

As introduced in an earlier lecture, the WRF-ARW model uses a terrain-following vertical coordinate η that is defined primarily as a function of dry hydrostatic pressure (i.e., the pressure of dry air under hydrostatic balance):

$$\eta = \frac{p_{dh} - p_{dht}}{p_0 - p_{dht}} + B(\eta)\left[1 - \frac{p_{dhs} - p_{dht}}{p_0 - p_{dht}}\right] \text{ (where } 0 \le \eta \le 1)$$

In the above, p_{dh} is the dry hydrostatic pressure, p_{dht} is the dry hydrostatic pressure at the top of the model (generally a user-defined parameter), p_{dhs} is the dry hydrostatic pressure at the surface, p_0 is a reference sea-level pressure, and $B(\eta)$ defines the relative weighting between a purely isobaric vertical coordinate and a terrain-following vertical coordinate. At locations where $p_{dhs} \sim p_0$ (where the surface is near sea-level), the vertical coordinate reduces to the first right-hand side term in the equation above. In all cases, η is 0 at the top of the model (where $p_{dh} = p_{dht}$ and $B(\eta) = 0$) and 1 at the surface (where $p_{dh} = p_{dhs}$ and $B(\eta) = 1$).

Because surface pressure can change through a model simulation, there exists a slight preference to height-based rather than pressure-based terrain-following vertical coordinates. However, most modern models use pressure-based terrain-following vertical coordinates. Examples include the WRF-ARW, RAP/HRRR (both currently WRF-ARW-based), GFS, NAM, and ECMWF models. Representative examples of models that use height-based vertical coordinates include the CM1 and MPAS models.

Models that use terrain-following vertical coordinates typically allow non-uniform vertical level distribution, so that our first consideration related to the choice of vertical coordinate is met. Fig.

5 depicts an example of pressure-based terrain-following vertical coordinate surfaces distributed between the terrain surface and the model top. The terrain-following coordinate surfaces means that our second consideration related to the choice of vertical coordinate is also met.

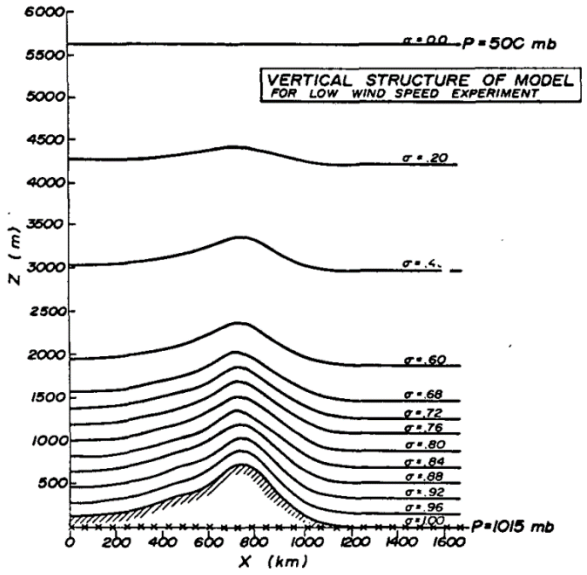

Figure 5. Cross-section of terrain-following pressure-based vertical coordinate surfaces for p_t = 500 hPa. Figure reproduced from Warner et al. (1978, *Mon. Wea. Rev.*), their Fig. 9.

This leaves only our third consideration, the computation of the horizontal pressure gradient. The generalized form of the transform operator between constant height z and terrain-following σ surfaces takes the form:

$$\nabla_\sigma(\ ) = \nabla_z(\ ) + \frac{\partial(\ )}{\partial z}\nabla_\sigma z$$

where subscripts of z and σ indicate the coordinate surface on which the quantity is evaluated. The original and transformed versions of the horizontal pressure gradient term in the u-momentum equation for the terrain-following pressure-based vertical coordinate used by the WRF-ARW model were given above and are reproduced below for convenience:

$$-\frac{1}{\rho}\frac{\partial p}{\partial x}_z$$

(constant height)

$$-\alpha\mu_d\frac{\partial p}{\partial x}_\eta - \frac{\alpha}{\alpha_d}\frac{\partial p}{\partial \eta}\frac{\partial \Phi}{\partial x}_\eta$$

(terrain-following, coupled to the dry air mass)

After the basic conversion to the terrain-following vertical coordinate, the second term was further manipulated to arrive at the form depicted above at right. Similar results would be obtained if a height-based terrain-following vertical coordinate were used or if a different model's formulation of the governing equations were considered.

Horizontal changes in pressure p and geopotential Φ along the terrain-following coordinate surface are particularly large in the presence of sharp horizontal gradients in terrain height. This can be understood given the definitions of pressure (related to the weight of the air above you) and the geopotential (related to the geometric height z). Consequently, the horizontal pressure gradient can be comparatively large near sloped terrain, and thus truncation error arising due to computing two horizontal pressure gradient terms may also be large. As noted above, WRF-ARW and other models typically address this by recasting the relevant terms into perturbation form to reduce the truncation error's magnitude.

It is also possible to devise a terrain-following vertical coordinate that is a function of potential temperature. Generally speaking, such vertical coordinates are terrain-following near the surface and transition to isentropic surfaces at some specified distance above the terrain. However, with a few exceptions – the now-replaced RUC model being one notable exception – terrain-following isentropic-based vertical coordinates are not used in modern models.

Variable Vertical Grid Resolution

Most modern models use variable grid resolution in the vertical. This is typically achieved with smaller vertical grid spacing near the ground (and sometimes near the tropopause) and larger vertical grid spacing elsewhere. An example is given in Fig. 6. However, some numerical models allow for variable grid resolution between domains, with more vertical levels and reduced spacing between levels on the inner nests. This helps maintain consistency between horizontal and vertical grid increments where other means of variable grid resolution would not.

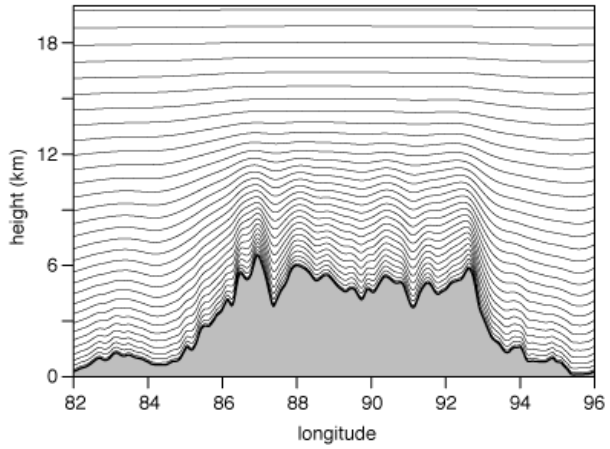

Figure 6. An example of a hybrid terrain-following vertical coordinate over a region of sloped topography. In this example, which is representative of the vertical coordinate in the Model for Prediction Across Scales, vertical levels follow the terrain below approximately 12 km above sea level. At higher altitudes, vertical levels closely resemble constant height surfaces. Image obtained from https://mpas-dev.github.io/.

The Consistency Between Horizontal and Vertical Grid Spacing

Greater attention has historically been given to the horizontal grid spacing and how well it is able to faithfully represent a feature or features of interest. However, we know that features such as cold and warm fronts on synoptic scales, cold pools, density currents, and inversions on the mesoscale, and gravity and inertia-gravity waves on the meso- to microscales slope horizontally with height. We want these sloping features to be represented smoothly on the model's grid. If a feature is insufficiently resolved in the vertical relative to its horizontal representation, the model may generate spurious gravity waves to try to balance the feature in the model.

The atmospheric dynamics for a given phenomenon can be used to help determine the best vertical grid spacing for that feature. For example, at midlatitudes, the vertical grid spacing needed to vertically resolve a feature can be related to the horizontal grid spacing by the following expression (Pecnick and Keyser 1989, *Meteor. Atmos. Phys.*):

$$\frac{\Delta z}{\Delta x} \leq s$$

where s is the vertical slope of an atmospheric phenomenon to be studied, such as a front. For the example of a front, as well as many other phenomena, s is ~0.005 to ~0.02 (e.g., rise 1 km for every 50 km to 200 km in the horizontal). This equation states that the slope of the model grid (given by $\Delta z/\Delta x$) should be less than or equal to the slope of the feature the model grid needs to resolve – which is rather intuitive.

The slope *s* of a given feature can be estimated from observations (e.g., vertical cross-sections) or may be estimated from dynamical principles. For example, *s* can be estimated from the ratio of the atmospheric scale height ($\Delta z \sim H_0$) to the Rossby radius of deformation ($\Delta x \sim \Delta L$; see also Lindzen and Fox-Rabinovitz 1989, *Mon. Wea. Rev.*):

$$\frac{\Delta z}{\Delta x} \leq \frac{f}{N}$$

In the above, *f* is the Coriolis parameter and *N* is the Brunt-Väisälä frequency, a measure of static stability.

Consider a simulation that contains a cold front somewhere in its domain. Let us assume that the slope *s* is equal to 0.01 for this front and that Δx is 20 km. Per the above equation, Δz then should be equal to 0.2 km, or 200 m. For a model domain with a model top at 20 km AGL, this suggests that 100 vertical levels are required to appropriately resolve the cold front. However, most models with $\Delta x \sim 20$ km typically use 30-80 vertical levels. Thus, one might conclude that the vertical grid spacing used in most simulations is too coarse, and this is true to a point. However, because most models use a variable vertical grid spacing, with finer spacing in regions where the sharpest vertical gradients typically exist (which, for a cold front, tend to be near the surface), the discrepancy between the chosen horizontal and vertical grid spacings is not as large as the initial evaluation would suggest.

Alternatively, so long as the model can faithfully represent the underlying dynamics, one may evaluate the model's kinetic energy spectrum to identify the vertical grid spacing below which the kinetic-energy spectrum does not significantly change. In the literature, this is referred to as *convergence*. A representative example is given by Fig. 7. For the model used ($\Delta x = 15$ km), a vertical grid spacing of 200 m is the vertical grid spacing at which convergence occurs. At coarser Δz, sloping atmospheric features are insufficiently resolved, resulting in spurious gravity waves that transfer kinetic energy from larger scales (evidenced by the red and black lines lying below the green and blue lines on the synoptic scale) to smaller scales whereupon the kinetic energy is dampened.

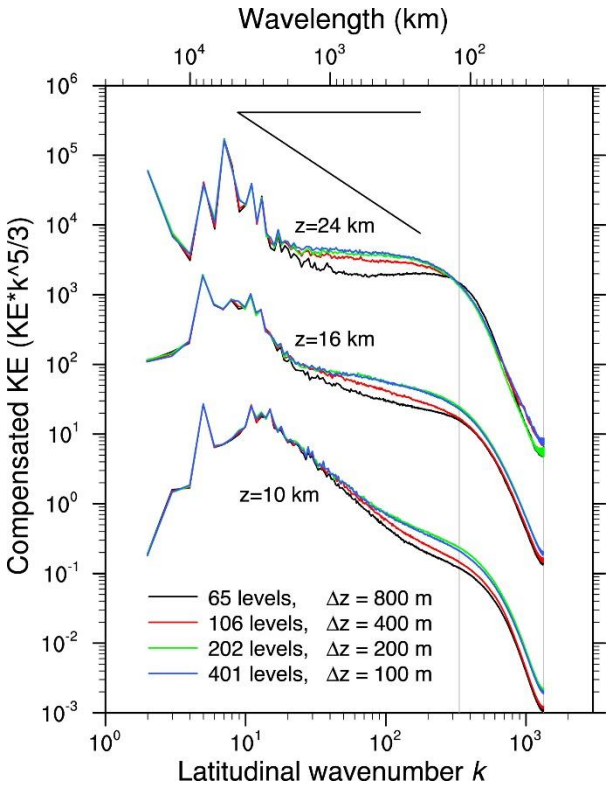

Figure 7. Kinetic energy times the latitudinal wavenumber *k* raised to the 5/3rd power (*y*-axis) as a function of latitudinal wavenumber *k* (inversely related to wavelength; smaller *k* indicates larger wavelength) at three altitudes (z = 10 km, 16 km, 24 km) from Δx = 15 km, day 6-7 global forecasts from the Model for Prediction Across Scales. Outputs from forecasts with vertical grid spacings of 800 m, 400 m, 200 m, and 100 m are given by the black, red, green, and blue curves, respectively. Note the similarity between the green and blue curves at each altitude, indicating convergence of the kinetic-energy spectra. Figure reproduced from Skamarock et al. (2019, *Mon. Wea. Rev.*), their Fig. 2.

Spurious gravity waves are generated when insufficient vertical resolution is used. These spurious waves superpose on the physical solution and degrade forecast quality. Consider Fig. 8. In Fig. 8a, where an appropriate vertical grid spacing is used, the model solution is smooth. In Fig. 8b, which differs from Fig. 8a only in that a vertical grid spacing that is three times coarser is used, the model solution is contaminated by spurious gravity waves. When the horizontal grid spacing is also coarsened, as in Fig. 8c, a smooth solution is obtained, but with reduced amplitude compared to Fig. 8a because of the coarsened horizontal grid.

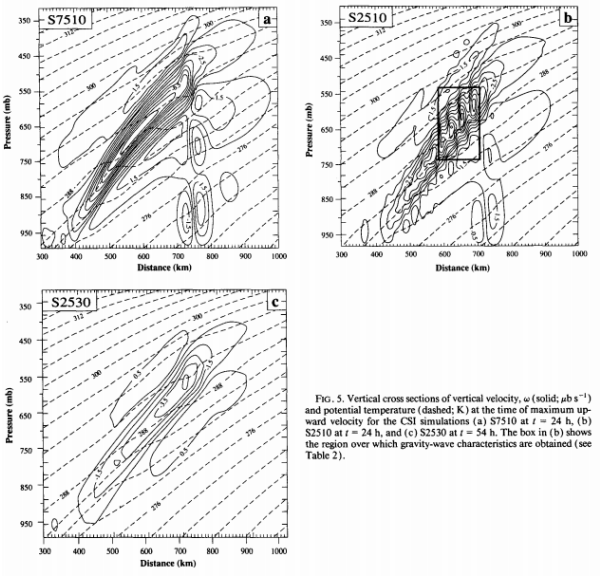

FIG. 5. Vertical cross sections of vertical velocity, ω (solid; μb s⁻¹) and potential temperature (dashed; K) at the time of maximum upward velocity for the CSI simulations (a) S7510 at t = 24 h, (b) S2510 at t = 24 h, and (c) S2530 at t = 54 h. The box in (b) shows the region over which gravity-wave characteristics are obtained (see Table 2).

Figure 8. Vertical cross-sections (x, p) of vertical velocity ω (solid lines, μbar s^{-1}) and potential temperature θ (dashed lines, K) at the time of maximum upward velocity from three numerical simulations of a case of conditional symmetric instability (a slantwise instability): (a) Δx = 10 km, 75 vertical levels; (b) Δx = 10 km, 25 vertical levels; and (c) Δx = 30 km, 25 vertical levels. In (b), note the high-frequency wave structure in the vertical velocity field, indicative of gravity waves, with no such structure in (a) and (c). In (c), the model's coarser resolution contributes to weaker vertical velocities compared to (a) and (b). Figure obtained from Persson and Warner (1991, *Mon. Wea. Rev.*), their Fig. 5.

Upper Boundary Conditions

Numerical models generally do not simulate the atmosphere's full depth; i.e., from the surface to where p = 0 hPa. Rather, the atmosphere's depth is typically truncated to a stratospheric isobaric surface. However, vertically propagating internal gravity waves, such as may be generated by intense thunderstorm updrafts impinging on the tropopause or by flow passing over sloped terrain, can propagate over a large vertical distance and potentially reach the model's top. What, then, should happen as these internal gravity waves reach the model's uppermost limit?

Most modern models use a rigid lid to represent the boundary at the top of the model atmosphere. This requires specifying an appropriate upper boundary condition. In the WRF-ARW model, this is often specified by the input meteorological data. However, this level is generally not at or close to the top of the atmosphere. This can pose a problem for radiation parameterizations, which must account for radiative transfer between the top of the atmosphere and the top of the model atmosphere. The most common approach for handling this is to assume a layer with thickness equal to the distance between the top of the modeled and actual atmospheres, though parameterizations differ in terms of how to specify the atmospheric

conditions over this layer (e.g., should values be uniform over this layer, possibly matching those at the top of the model atmosphere, or should they vary, possibly linearly between the top of the model atmosphere and a top-of-atmosphere climatology?). More details on upper boundary specification in the context of radiation parameterizations can be found in Cavallo et al. (2011, *Mon. Wea. Rev.*).

Using a rigid lid at the top of the model atmosphere means that, in theory, vertically propagating waves can be reflected by the rigid upper boundary. To mitigate the non-physical reflection of vertically propagating waves as they impinge on the rigid lid, an absorbing or damping layer can be added to the top of the model atmosphere. There are many forms for this layer, with the two most common being viscous and Rayleigh damping.

Viscous damping involves defining an absorbing layer in the upper reaches of the model. In this layer, the eddy viscosity coefficients K_h (horizontal) and K_v (vertical) have default values at the bottom of the layer that increase to a specified maximum value at the top of the layer. Eddy-viscosity coefficients reduce horizontal and/or vertical gradients of meteorological fields where they exist in the model atmosphere. The influence of a viscous damping layer of 20-km depth in a model with a top at z = 50 km is depicted in Fig. 9.

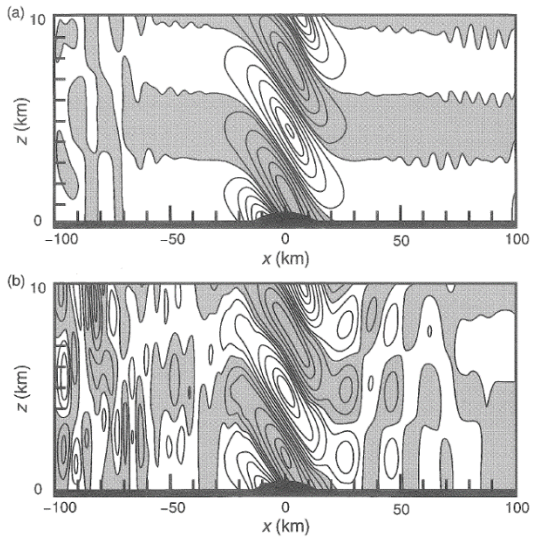

Figure 9. Vertical motion (contours; negative values shaded) from 2-D model simulations of flow over elevated topography (dark shading at bottom) for simulations with (a) a viscous damping layer of 20 km depth at the top of the model and (b) no viscous damping. Figure reproduced from Warner (2011), their Fig. 3.50.

The viscous damping option available within the WRF-ARW model takes the following form, as documented in section 4.4.1 of Skamarock et al. (2019):

$$K_{dh} = \frac{\Delta x^2}{\Delta t}\gamma_g \cos\left(\frac{\pi}{2}\frac{z_{top} - z}{z_d}\right) \qquad \text{(horizontal)}$$

$$K_{dv} = \frac{\Delta z^2}{\Delta t}\gamma_g \cos\left(\frac{\pi}{2}\frac{z_{top} - z}{z_d}\right) \qquad \text{(vertical)}$$

In the above, the K_{dh} and K_{dv} are the eddy viscosity coefficients applicable in the damping layer; γ_g is a user-specified nondimensional damping coefficient, z_{top} is the height of the model top, and z_d is the damping layer's depth. The recommended values for γ_g range between 0.01 and 0.1 and the default value for z_d is 5 km. At the model's top, where $z = z_{top}$, the cos functions equal 1. At the bottom of the damping layer, where $z_{top} - z = z_d$, the cos functions equal 0.

Rayleigh damping involves defining an absorbing layer in the upper portions of the model. Here, however, model variables are relaxed (or nudged) toward a pre-defined reference state. For any model variable α, a generic formulation for a Rayleigh damping operator takes the form:

$$\frac{\partial \alpha}{\partial t} = -\tau(z)\left(\alpha - \bar{\alpha}\right)$$

Here, the time tendency of α is a function of the damping operator τ (which is a function of height z) and the departure of α from its reference-state value $\bar{\alpha}$.

The WRF-ARW model contains a form of this Rayleigh damping, as documented in section 4.4.3 of Skamarock et al. (2019):

$$\frac{\partial u}{\partial t} = -\tau(z)\left(u - \bar{u}\right) \qquad \frac{\partial v}{\partial t} = -\tau(z)\left(v - \bar{v}\right) \qquad \frac{\partial \omega}{\partial t} = -\tau(z)\omega \qquad \frac{\partial \theta}{\partial t} = -\tau(z)\left(\theta - \bar{\theta}\right)$$

Reference-state fields are functions of only z. The reference-state vertical velocity is assumed to be zero. Because the heights of the vertical coordinate surfaces in the WRF-ARW model change with time (since they are based on pressure), the reference-state values on model coordinate surfaces must be adjusted accordingly at each time step.

The Rayleigh damping function takes the form:

$$\tau(z) = \gamma_d \sin^2\left[\frac{\pi}{2}\left(1 - \frac{z_{top} - z}{z_d}\right)\right]$$

where the Rayleigh damping is applied only over the damping layer depth specified by z_d. γ_d is a user-specified damping coefficient with a recommended value approximately equal to 0.003 s^{-1}.

At the model's top, where $z = z_{top}$, the $\sin^2$ function is equal to 1 and damping takes its maximum value of $-\gamma_r\left(\alpha - \overline{\alpha}\right)$. At the bottom of the damping layer, where $z_{top} - z = z_d$, the $\sin^2$ function is equal to 0 and damping is not applied.

It is also possible to apply an implicit Rayleigh damping only to the vertical velocity. In this formulation, the Rayleigh damping is applied to the perturbation vertical velocity during the model's integration. It influences the coupled vertical velocity W and, given that W appears in its definition, the geopotential Φ. This implicit Rayleigh damping takes the form given by equation (4.14) of Skamarock et al. (2019):

$$W'' = \widetilde{W}'' - \tau(z)\Delta\tau W''$$

Here, τ has the same form as for the traditional Rayleigh damping, albeit with a recommended value of γ_d of approximately 0.2 s^{-1}. $\widetilde{W}''$ is the value of W'' at the end of the acoustic time step while W'' is its value prior to the acoustic time step. This formulation is akin to including an implicit damping term in the vertical momentum equation and adding implicit vertical diffusion to the vertical velocity. Klemp et al. (2008, *Mon. Wea. Rev.*) should be consulted for more information regarding this formulation.

Finally, there are two other ways in which the model's top may be represented, although each are typically not used in modern models: representing the model's top by a free surface across which there is no flow, or representing the model's top by a radiative boundary condition, wherein the energy associated with vertically propagating waves is permitted to be radiated upward and out of the simulation domain. The former require an absorbing or damping layer whereas the latter do not. See Klemp and Durran (1983, *Mon. Wea. Rev.*) for more details regarding radiative boundary condition formulations.